

K.L. He, X.H. Mo, P. Wang, and C.Z. Yuan  
*Institute of High Energy Physics, CAS, Beijing 100049, China*  
 (Dated: February 13, 2006)

The previous experiments which provide information on the  $\psi(3770)$  to non- $D\bar{D}$  decays are reviewed. Three approaches of searching for the non- $D\bar{D}$  decays are discussed in detail. It is also pointed out that the search for the non- $D\bar{D}$  decays of the  $\psi(3770)$  is very important for the understanding of the dynamics of charmonium decays.

PACS numbers: 13.25.Gv, 12.38.Qk, 14.40.Gx

## I. INTRODUCTION

The lowest charmonium resonance above the charmed particle production threshold is  $\psi(3770)$  (shortened as  $\psi''$ ) which provides a rich source of  $D^0\bar{D}^0$  and  $D^+D^-$  pairs, as anticipated theoretically [1]. However, non- $D\bar{D}$  decays of the  $\psi(3770)$  was also expected theoretically and was searched for experimentally almost two decades ago. The OZI violation mechanism [2] was utilized to understand the possibility of the non- $D\bar{D}$  decays of the  $\psi(3770)$  [3], and the pioneer experimental investigations of the non- $D\bar{D}$  decay modes could be found in Ref. [4].

After a period of silence, the study of the non- $D\bar{D}$  decays of the  $\psi''$  gets renaissance as more and more data are collected at  $\psi''$  by BES-II and CLEOc [5]. Extensive studies have been made for exclusive non- $D\bar{D}$  decay channels [6–10], of which the most prominent one is the hadronic transition of  $\psi'' \rightarrow J/\psi\pi^+\pi^-$  once sought by Mark-III [4]. Recently both BES and CLEOc collaborations reported their measurements for this channel [11, 12], which are in marginally agreement with each other. However, except for  $J/\psi\pi^+\pi^-$  final state, no statistically significant signals of the non- $D\bar{D}$  decays at  $\psi''$  are presented up till now. One possible reason is that the existing data samples are still not large enough to search for the channels of such small branching fractions.

Besides the searches for the exclusive modes, there is the search for inclusive decays. In fact, the indication of a substantial non- $D\bar{D}$  decays of the  $\psi''$  was originally caught attention from the comparison of the cross sections of the inclusive hadrons and  $D\bar{D}$  at the  $\psi''$  peak. Table I summarizes the measurements of the resonance parameters and the observed cross section of the inclusive hadronic decay, and Table II summarizes the measurements of the  $D\bar{D}$  cross section reported by BES-II [13] and CLEOc [14] collaborations using either double-tag or single-tag method. The simple average of the values in the two tables gives  $\sigma^{obs}(\psi'') \simeq 7.75$  nb and  $\sigma(D\bar{D}) \simeq 6.27$  nb, respectively, with difference of about 1.5 nb (about 19% of the total cross section of the  $\psi''$  production), which implies the non- $D\bar{D}$  decays of the  $\psi''$  is important. However, the existence of substantial non- $D\bar{D}$  decays is not unambiguous due to the poor statistics of the data samples and the complexity of the analysis. In addition, results from different experiments are con-

sistent with each other only marginally. Moreover, for inclusive measurement, the contribution of the non- $D\bar{D}$  decays has been neglected in previous experiments in measuring the  $\psi''$  resonance parameters.

Besides the experimental motivations, there are interests to look into this problem from the theoretical point of view. In Ref. [20], it is estimated that at most 600 keV ( $\sim 2.5\%$ ) of the  $\psi''$  total width of  $(23.6 \pm 2.7)$  MeV is due to the radiative transition, and perhaps as much as another 100 keV ( $\sim 0.4\%$ ) is due to the hadronic transition to  $J/\psi\pi\pi$ . All these together are far from accounting for a deficit of 19% of the total  $\psi''$  width.

In a most recent paper [22], based on the available experimental information of  $J/\psi$  and  $\psi'$  decays, it is estimated that the charmless decay of  $\psi''$  by virtue of the  $S$ - and  $D$ -wave charmonia mixing scheme [23] could be as large as 3.1 MeV or 13% of the total decay width of  $\psi''$ . By charmless decay, we exclude those decay modes with either open or hidden charm. If we take into account also the charmonium transition contributions of 3% [20] (2.5% for radiative transition and 0.34% for  $J/\psi\pi\pi$ ), the total non- $D\bar{D}$  decay of  $\psi''$  as large as 16% is conceivable in the  $2S$ - $1D$  mixing scenario.

With the expected more data at  $\psi''$  from the running CLEOc, it is feasible to search for the possible large non- $D\bar{D}$  decays. Furthermore, we notice that the accurate determination of certain exclusive final state can supply the knowledge of the phase between the  $S$ -wave and  $D$ -wave matrix elements. Such information can provide some clues concerning the dynamics of the OZI suppressed decays of charmonium.

In this paper, we concentrate on the experimental aspects of the non- $D\bar{D}$  decays of the  $\psi''$ . In the following sections, we discuss the exclusive, the quasi-inclusive and the inclusive methods for the non- $D\bar{D}$  searching, especially, we shall expound some of the technique details in the handling of the experimental data which were overlooked in previous measurements.

## II. EXCLUSIVE METHOD

One may measure the branching fraction of each individual charmless decay mode. If  $\psi''$  is produced in  $e^+e^-$  collision, the nonresonance continuum amplitude could be important, its contribution, and its interference with

TABLE I: Resonance parameters and total cross sections at  $\psi''$ .  $\Gamma_{\psi''}$  is the full width,  $\Gamma_{ee}$  the partial width to electron pairs,  $\sigma^{obs}$  the observed cross section at resonance peak,  $R_{flat}$   $R$  value to describe the continuum contribution,  $\sigma^{Born}$  Born order cross section. It should be noticed that the uncertainty of  $\sigma^{Born}$  is obtained from those of the quantities used for calculation without considering the correlation among them.

Experiment/ Accelerator	$M_{\psi''}$ (MeV/ $c^2$ )	$\Gamma_{\psi''}$ (MeV/ $c^2$ )	$\Gamma_{ee}$ (eV/ $c^2$ )	$\sigma^{obs}$ (nb)	$R_{flat}$	$\sigma^{Born}$ (nb)	$\sigma^{obs}/\sigma^{Born}$
LGW/SPEAR [15]	$3772 \pm 6$	$28 \pm 5$	$370 \pm 90$	$10.3 \pm 2.1$	$\sim 2.8^a$	$13.6 \pm 4.1$	0.75
DELCO/SPEAR [16]	$3770 \pm 6$	$24 \pm 5$	$180 \pm 60$	$\sim 6.1^a$	$\sim 2.5^a$	$7.7 \pm 3.0$	0.79
MARKII/SPEAR [17]	$3764 \pm 5$	$24 \pm 5$	$276 \pm 50$	$9.3 \pm 1.6$	$2.22 \pm 0.06$	$11.9 \pm 3.3$	0.78
CBAL/SPEAR [18]	$3768 \pm 2$	$34 \pm 8$	$283 \pm 70$	$6.7 \pm 0.9$	$2^b$	$8.6 \pm 2.9$	0.78
BESII/BEPC [19]	$3773 \pm 1$	$26 \pm 4$	$247 \pm 35$	$\sim 6.4^a$	$2.44 \pm 0.08$	$9.8 \pm 2.0$	0.65
BESII/BEPC [20, 21]	3772	23.2	—	$7.7 \pm 1.1$	$\sim 2.16^a$	$12.1 \pm 1.9^c$	0.64

<sup>a</sup> The value estimated from the corresponding figure provided by literature or thesis, only for reference.

<sup>b</sup> The  $R$  is only treated as constant in the fitting.

<sup>c</sup> Absent values are adopted from PDG for calculating  $\sigma^{Born}$ .

TABLE II: Comparison of cross sections  $\sigma(D\bar{D}) \equiv \sigma(e^+e^- \rightarrow \psi'' \rightarrow D\bar{D})$ , in nb. Note that  $\sigma(D^0)$  is defined to be twice  $\sigma(D^0\bar{D}^0)$  and  $\sigma(D^+)$  is twice  $\sigma(D^+D^-)$ .

Collaboration	$\sqrt{s}$ (GeV)	$\sigma(D^+)$	$\sigma(D^0)$	$2\sigma(D\bar{D})$
MARKIII[? ]	3.768	$3.35^{+0.44}_{-0.36} \pm 0.24$	$4.48^{+0.33}_{-0.29} \pm 0.37$	$7.83^{+0.55}_{-0.46} \pm 0.52$
MARKIII[? ]	3.768	$4.2 \pm 0.6 \pm 0.3$	$5.8 \pm 0.5 \pm 0.6$	$10.0 \pm 0.8 \pm 0.8$
	$\sqrt{s}$ (GeV)	$\sigma(D^+D^-)$	$\sigma(D^0\bar{D}^0)$	$\sigma(D\bar{D})$
BESII <sup>a</sup> [13]	3.773	$2.52 \pm 0.07 \pm 0.23$	$3.26 \pm 0.09 \pm 0.26$	$5.78 \pm 0.11 \pm 0.38$
CELO <sup>a</sup> [14]		$2.58 \pm 0.15 \pm 0.19$	$3.90 \pm 0.42 \pm 0.28$	$6.48 \pm 0.44 \pm 0.49$

<sup>a</sup> Preliminary

the  $\psi''$  decay amplitude must be considered in the analysis of the experimental data [24]. This was discussed in detail for the vector-pseudoscalar (VP) modes [25], in which the observed cross section depends on the interference pattern between the  $\psi''$  amplitude and the continuum amplitude. If the phase between the strong and electromagnetic interactions is  $-90^\circ$ , as suggested in Ref. [26], such interference is destructive for  $\rho\pi$ ,  $\omega\eta$ ,  $\omega\eta'$ ,  $K^{*+}K^-$ ,  $b_1\pi$  and  $K^+K^-$  modes but constructive for  $\phi\eta$ ,  $\phi\eta'$  and  $K^{*0}\bar{K}^0$  modes. Destructive interference between the resonance and continuum means that the observed cross section on top of the resonance could be smaller than the continuum cross section. The experimental results on  $\rho\pi$  and  $\omega\eta$  modes[8] demonstrate this interference pattern.

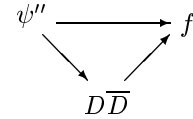
As a matter of fact, many subtleties concerning the efficiency determination and Monte Carlo simulation have to be taken into consideration in order to acquire correct and accurate measurement of the exclusive decay at the  $\psi''$  peak in  $e^+e^-$  experiments. A furthermore expound of such measurement is presented in Ref. [27].

### III. QUASI-INCLUSIVE METHOD

The exclusive method gives the branching fraction of each individual charmless decay mode, but provides no information on the total fraction of the non- $D\bar{D}$  decays.

In this section, we develop a quasi-inclusive method, by which we can derive the total non- $D\bar{D}$  decay branching fraction from the inclusive measurement of certain particle or final state.

Certain final state  $f$  may be produced from the direct  $\psi''$  decays, and/or from the cascade  $D\bar{D}$  decays, as shown below:



The following quantities are needed to describe such a process in detail

- $\mathcal{B}(\psi'' \rightarrow f)$ : the total branching fraction of final state  $f$  in  $\psi''$  decay;
- $\mathcal{B}(\psi'' \rightarrow D\bar{D})$ : the branching fraction of  $D\bar{D}$  in  $\psi''$  decays;
- $\mathcal{F}(D\bar{D} \rightarrow f)$ : the branching fraction of final state  $f$  in  $D\bar{D}$  decay;
- $\bar{\mathcal{B}}(D\bar{D} \rightarrow f)$ : the branching fraction of final state  $f$  from non- $D\bar{D}$   $\psi''$  decay (direct  $\psi''$  decays).

So we have the following relation

$$\begin{aligned} \mathcal{B}(\psi'' \rightarrow f) &= \mathcal{B}(\psi'' \rightarrow D\bar{D}) \cdot \mathcal{F}(D\bar{D} \rightarrow f) \\ &+ \bar{\mathcal{B}}(D\bar{D} \rightarrow f). \end{aligned} \quad (1)$$

According to the above relation, in order to find out  $\mathcal{B}(\psi'' \rightarrow D\bar{D})$ , or equivalently  $[1 - \mathcal{B}(\psi'' \rightarrow D\bar{D})]$ , we need to know  $\mathcal{B}(\psi'' \rightarrow f)$ ,  $\mathcal{F}(D\bar{D} \rightarrow f)$  and  $\bar{\mathcal{B}}(D\bar{D} \rightarrow f)$ . So we first discuss how to determine these branching fractions experimentally.

### A. Determing $\mathcal{F}(D\bar{D} \rightarrow f)$

The D meson decay branching fraction ( $\mathcal{F}_i$ ) was originally measured through the production ( $\sigma_D \cdot \mathcal{F}_i$ ), then converted into D decay branching fraction ( $\mathcal{F}_i$ ) by employing the cross section  $\sigma_D$  at  $\psi''$  peak [15, 28]. Unfortunately, as indicated in Table I, there are large discrepancies among the measurements of  $\sigma_D$ . Furthermore, in previous measurements  $\psi''$  was assumed solely or substantially decay into  $D\bar{D}$ , which is questionable. We will return to this point in detail in section IV.

Twenty years ago, a new technique was developed by MARK III group [29] to derive the D meson branching fraction without relying on the measurement of the D-production cross section. To determine the indivial branching fraction ( $\mathcal{F}_i$ ), together with the number of produced  $D\bar{D}$  pairs ( $N$ ), the corrected number of single tags ( $S_i$ ) and double tags ( $D_{ij}$ ) are employed in a  $\chi^2$  minimization fit, using the following expressions:

$$\begin{aligned} S_i &= 2N\mathcal{F}_i\epsilon_i - 2N \sum_j \mathcal{F}_i\mathcal{F}_j\alpha_{ij}^i; \\ D_{ij} &= \begin{cases} 2N\mathcal{F}_i\mathcal{F}_j\epsilon_{ij} & (i \neq j) \\ N\mathcal{F}_i^2\epsilon_{ii} & (i = j) \end{cases}, \end{aligned}$$

where  $\epsilon_i$  is the efficiency for reconstructing a single tag in the  $i$ th  $D$  decay mode,  $\epsilon_{ij}$  is the efficiency for reconstructing a double tag for  $D\bar{D}$  decay mode  $i$  and  $j$ , and  $\alpha_{ij}^i$  is the efficiency for reconstructing a single tag of mode  $i$  while simultaneously reconstructing the entire event as a double tag of mode  $i$  and  $j$ . The second term in the expression for  $S_i$  removes from the single-tag sample those tags which also appear in the double-tag sample. This subtraction leaves the two samples independent and eliminates the directly correlated errors. Comparing the number of observed single tage ( $S_i$ ) events with double tags ( $D_{ij}$ ) events yields the branching fraction of decay mode  $j$  without referring to the production cross section. In practice, the  $S_i$  serves to determine the relative branching fractions, while the  $D_{ij}$  sets the absolute scale of the branching fractions.

By virtue of the approach introduced above, we obtain  $\mathcal{F}(D\bar{D} \rightarrow f)$  for a final state  $f$  without measuring production cross section. In fact, any measured results of  $\mathcal{F}(D\bar{D} \rightarrow f)$  by the approach can be used for the following analysis even if the results are from different experimental groups.

### B. Determing $\mathcal{B}(\psi'' \rightarrow f)$ and $\bar{\mathcal{B}}(D\bar{D} \rightarrow f)$

The  $\mathcal{B}(\psi'' \rightarrow f)$  is obtained by scan experiments. Avoiding abstract, we take the inclusive  $K_S$  final state as example to explain the scan process.

Usually at least two scan curves are needed, one is the inclusive hadron final state, from which we determine the total decay width of  $\psi''$  ( $\Gamma_t$ ); the other is the inclusive  $K_S$  final state ( $K_S$  plus anything), from which we determine the partial decay width of this inclusive mode. The ratio of these two widths give the branching fraction  $\mathcal{B}(\psi'' \rightarrow K_S + \text{anything})$ .

At the energy in the vicinity of  $\psi''$ , besides the  $\psi''$  resonance, there are other cross sections due to the non-resonance continuum process as well as the tails of the  $J/\psi$  and  $\psi'$ , which together account for a large proportion of the measured cross section at the  $\psi''$  peak. According to the decay topology, the inclusive hadron events are divided into two categories, the  $D\bar{D}$  events and the  $D\bar{D}$ -less final states. Here we coin a word “ $D\bar{D}$ -less final states” to depict all the processes which do not go through  $D$  or  $\bar{D}$ , including non-resonance process, tails of  $J/\psi$  and  $\psi'$ , and the non- $D\bar{D}$  decays of the  $\psi''$ . By non- $D\bar{D}$  decay, we mean the  $\psi''$  decays which do not go through  $D$  or  $\bar{D}$ . Here the correct Monte Carlo simulation deserves special attention. For example, the non-resonance continuum process can be simulated by Lund model [30]; while the  $J/\psi$ ,  $\psi'$  tails and  $D\bar{D}$  decay by the Monte Carlo which describes  $J/\psi$ ,  $\psi'$  and  $D$  decays respectively [31, 32]. The synthetic hadron efficiency  $\epsilon_{had}$  is expressed as

$$\epsilon_{had}^{K_S} = \frac{\epsilon_{DL}^{K_S} \cdot \sigma_{DL}^{K_S} + \epsilon_{DD}^{K_S} \cdot \sigma_{DD}^{K_S}}{\sigma_{DL}^{K_S} + \sigma_{DD}^{K_S}}, \quad (2)$$

where  $\epsilon$  and  $\sigma$  denote the efficiencies and the corresponding cross sections, the subscript  $DL$  indicates the  $D\bar{D}$ -less decay, while  $DD$  the  $D\bar{D}$  decay, the subscript  $K_S$  represents the inclusive hadron final state containing  $K_S$  particle. However,  $\sigma_{DL}$  and  $\sigma_{DD}^{K_S}$  are to be determined from experiment. Fortunately, according to Eq. (2), what we need to know is the ratio of  $\sigma_{DL}$  to  $\sigma_{DD}^{K_S}$ , which could be acquired experimentally as explained below.

Fig. 1 shows the momentum distributions of the inclusive  $K_S$  events due to the  $D\bar{D}$  (histogram) and the  $D\bar{D}$ -less (dots with error bar) decays, which are simulated by DDGEN and Lund generators, respectively. With the two generators, we obtain the efficiencies  $\epsilon_{DL}$  and  $\epsilon_{DD}^{K_S}$ . For the real data sample, its momentum distribution is the synthetic one of the  $D\bar{D}$  and the  $D\bar{D}$ -less decays with certain proportion of each. We fit the data distribution with those of Monte Carlo distributions as shown in Fig. 1, then obtain the numbers of the observed events of these two processes, which are denoted as  $n_{DL}$  and  $n_{DD}^{K_S}$ . Utilizing the relation

$$n = L\sigma\epsilon \quad (L: \text{expriment luminosity}),$$

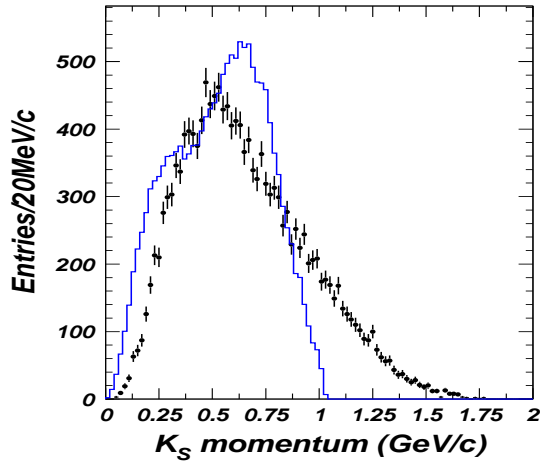


FIG. 1:  $K_S$  momentum distributions: histogram for inclusive  $K_S$  final state from  $D\bar{D}$  decays; dots with error bars for inclusive  $K_S$  final state from  $D\bar{D}$ -less decays.

we get

$$\frac{n_{DL} \cdot \epsilon_{DD}^{K_S}}{n_{DD}^{K_S} \cdot \epsilon_{DL}} = \frac{\sigma_{DL}}{\sigma_{DD}^{K_S}}. \quad (3)$$

In short, we determine  $\mathcal{B}(\psi'' \rightarrow f)$  by scan experiment. As to  $\overline{\mathcal{B}}(D\bar{D} \rightarrow f)$ , we notice that in Fig. 1, most of the momentum from  $D\bar{D}$  decay is less than 1 GeV, so a requirement of the momentum greater than 1.1 GeV eliminates all the  $D\bar{D}$  decay event, while leaving the events from  $D\bar{D}$ -less decay. Using such events, we obtain another scan curve. Fit this curve together with the curve of the total inclusive hadrons, we determine  $\overline{\mathcal{B}}(D\bar{D} \rightarrow f)$ . This process is similar to the determination of  $\mathcal{B}(\psi'' \rightarrow f)$ , but only one efficiency  $\epsilon_{DL}$  is needed.

### C. Deriving $\mathcal{B}(\psi'' \rightarrow D\bar{D})$

Since  $\mathcal{B}(\psi'' \rightarrow f)$ ,  $\mathcal{F}(D\bar{D} \rightarrow f)$  and  $\overline{\mathcal{B}}(D\bar{D} \rightarrow f)$  are obtained experimentally, by solving Eq. (1), we get  $\mathcal{B}(\psi'' \rightarrow D\bar{D})$ , then acquire the non- $D\bar{D}$  decay branching fraction  $[1 - \mathcal{B}(\psi'' \rightarrow D\bar{D})]$ .

Next we understand Eq. (1) from physics point of view. We introduce a new quantity defined as

$$\overline{\mathcal{F}}(D\bar{D} \rightarrow f) = \frac{\overline{\mathcal{B}}(D\bar{D} \rightarrow f)}{1 - \mathcal{B}(\psi'' \rightarrow D\bar{D})},$$

which is the ratio of the branching fraction of non- $D\bar{D}$  decay for the final state  $f$  to that of the total non- $D\bar{D}$  decays. Then Eq. (1) reads

$$\begin{aligned} \mathcal{B}(\psi'' \rightarrow f) &= \mathcal{B}(\psi'' \rightarrow D\bar{D}) \cdot \mathcal{F}(D\bar{D} \rightarrow f) \\ &+ [1 - \mathcal{B}(\psi'' \rightarrow D\bar{D})] \cdot \overline{\mathcal{F}}(D\bar{D} \rightarrow f). \end{aligned} \quad (4)$$

We chose  $\mathcal{B}(\psi'' \rightarrow f)$  as ordinate, and  $\mathcal{B}(\psi'' \rightarrow D\bar{D})$  as abscissa, which varies from 0 to 100%. For certain

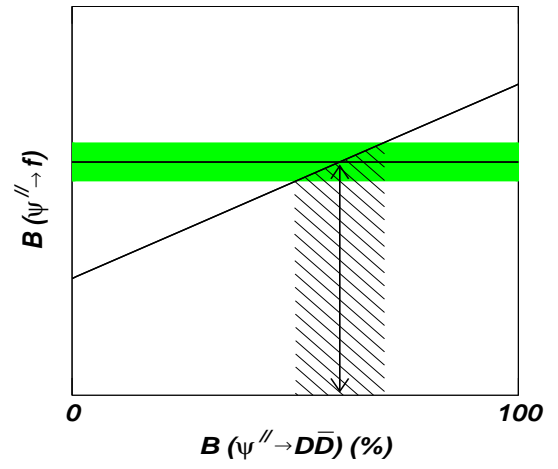


FIG. 2: Diagram for the determination of  $\mathcal{B}(\psi'' \rightarrow D\bar{D})$ . The horizontal line indicates a certain  $\mathcal{B}(\psi'' \rightarrow f)$  with shaded band as its uncertainty; the askew line is drawn based on information of  $\mathcal{B}(D\bar{D} \rightarrow f)$  and  $\overline{\mathcal{B}}(D\bar{D} \rightarrow f)$ ; the arrow indicates the  $\mathcal{B}(\psi'' \rightarrow D\bar{D})$  determined from experiment with hatched area as its uncertainty.

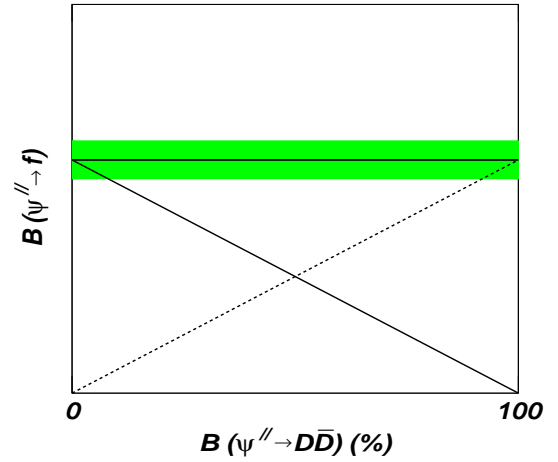


FIG. 3: Diagram for the determination of  $\mathcal{B}(\psi'' \rightarrow D\bar{D})$ . The horizontal line indicates a certain  $\mathcal{B}(\psi'' \rightarrow f)$  with shaded band as its uncertainty; the solid askew line corresponds to  $\mathcal{F}(D\bar{D} \rightarrow f) = 0$  for certain final state  $f$  while the dashed askew line corresponds to  $\overline{\mathcal{F}}(D\bar{D} \rightarrow f) = 0$  for certain final state  $f$ .

final state  $f$ ,  $\mathcal{B}(\psi'' \rightarrow f)$  corresponds to the horizontal line, as shown in Fig. 2, where the shaded band denotes the uncertainty of  $\mathcal{B}(\psi'' \rightarrow f)$ . If  $\mathcal{B}(\psi'' \rightarrow D\bar{D}) = 0$ , then  $\mathcal{B}(\psi'' \rightarrow f) = \overline{\mathcal{F}}(D\bar{D} \rightarrow f)$ , which means all events of final states  $f$  coming from non- $D\bar{D}$  decay; if  $\mathcal{B}(\psi'' \rightarrow D\bar{D}) = 100\%$ , then  $\mathcal{B}(\psi'' \rightarrow f) = \mathcal{F}(D\bar{D} \rightarrow f)$ , which means all events of final states  $f$  coming from  $D\bar{D}$  decay, or equivalently the complete absence of the contribution from non- $D\bar{D}$  decay. Without losing generality, we assume that  $\mathcal{F}(D\bar{D} \rightarrow f) > \overline{\mathcal{F}}(D\bar{D} \rightarrow f)$ , then we obtain an upward line in the coordinate, as shown in Fig. 2. Similarly, if we assume that  $\mathcal{F}(D\bar{D} \rightarrow f) <$

$\overline{\mathcal{F}}(D\overline{D} \rightarrow f)$ , we obtain a downward line in the coordinate. The point of interaction gives rise to the determination of  $\mathcal{B}(\psi'' \rightarrow D\overline{D})$ , which is denoted by the arrow in Fig. 2. The hatched area indicates the uncertainty of  $\mathcal{B}(\psi'' \rightarrow D\overline{D})$ , which is due to the interaction of the askew line with the uncertain band of  $\mathcal{B}(\psi'' \rightarrow f)$ . Here we notice that the smaller the slope of askew line in Fig. 2, the longer is the interaction line with the uncertainty band, which means the larger uncertainty in the determination of  $\mathcal{B}(\psi'' \rightarrow D\overline{D})$ . On the contrary, if the slope of the askew line is larger, we obtain comparatively smaller uncertainty on  $\mathcal{B}(\psi'' \rightarrow D\overline{D})$ . In another word, to obtain  $\mathcal{B}(\psi'' \rightarrow D\overline{D})$  as accurate as possible, we select those final states which have as large as possible the difference between  $\mathcal{F}(D\overline{D} \rightarrow f)$  and  $\overline{\mathcal{F}}(D\overline{D} \rightarrow f)$ .

One special case is that  $\mathcal{F}(D\overline{D} \rightarrow f) = \overline{\mathcal{F}}(D\overline{D} \rightarrow f)$ , according to Eq. (4), we have  $\mathcal{B}(\psi'' \rightarrow f) = \mathcal{F}(D\overline{D} \rightarrow f) = \overline{\mathcal{F}}(D\overline{D} \rightarrow f)$ . Under such circumstance, we can not get any information about the total non- $D\overline{D}$  decay. In another word, if the scan experiment obtains the  $\mathcal{B}(\psi'' \rightarrow f)$ , which is equal to  $\mathcal{F}(D\overline{D} \rightarrow f)$ , we could neither confirm nor deny the existence of non- $D\overline{D}$  decay. Another special case is  $\mathcal{F}(D\overline{D} \rightarrow f) = 0$  or  $\overline{\mathcal{F}}(D\overline{D} \rightarrow f) = 0$ . For example, for baryon anti-baryon ( $B\overline{B}$ ) final state, which does not come from  $D\overline{D}$  decays,  $\mathcal{F}(D\overline{D} \rightarrow f) = 0$ . Under such circumstance Eq. (1) becomes

$$\mathcal{B}(\psi'' \rightarrow f) = [1 - \mathcal{B}(\psi'' \rightarrow D\overline{D})] \cdot \overline{\mathcal{F}}(D\overline{D} \rightarrow f). \quad (5)$$

According to the above equation,  $\mathcal{B}(\psi'' \rightarrow f) = \overline{\mathcal{F}}(D\overline{D} \rightarrow f)$  for  $\mathcal{B}(\psi'' \rightarrow D\overline{D}) = 0$  while  $\mathcal{B}(\psi'' \rightarrow f) = 0$  for  $\mathcal{B}(\psi'' \rightarrow D\overline{D}) = 1$ . So mathematically, when  $\mathcal{B}(D\overline{D} \rightarrow f) = 0$ , Eq. (5) provides a downward line in coordinate as shown in Fig. 3, where the only point of interaction is at  $\mathcal{B}(\psi'' \rightarrow D\overline{D}) = 0$ . Physically, at the start point of abscissa in Fig. 3, Eq. (5) merely gives a fact that all the final states  $f$  events come from non- $D\overline{D}$  decay since its decay through  $D\overline{D}$  is forbidden. As for other values of  $\mathcal{B}(\psi'' \rightarrow D\overline{D})$ , we could not get any information because the two lines do not intersect.

If the uncertainties due to  $\mathcal{F}(D\overline{D} \rightarrow f)$  and  $\overline{\mathcal{F}}(D\overline{D} \rightarrow f)$  are taken into account, the askew lines in Fig. 2 and 3 become bands, just like the horizontal ones. Under such circumstance, all discussions above are valid except for the uncertainty of the determined  $\mathcal{B}(\psi'' \rightarrow D\overline{D})$ , which becomes larger.

#### IV. INCLUSIVE METHOD

In this section, we first retrospect the previous scan experiments, and point out drawbacks of these experiments, then put forth a new method which determines the inclusive non- $D\overline{D}$  decay directly with small systematic errors.

#### A. Scan experiment

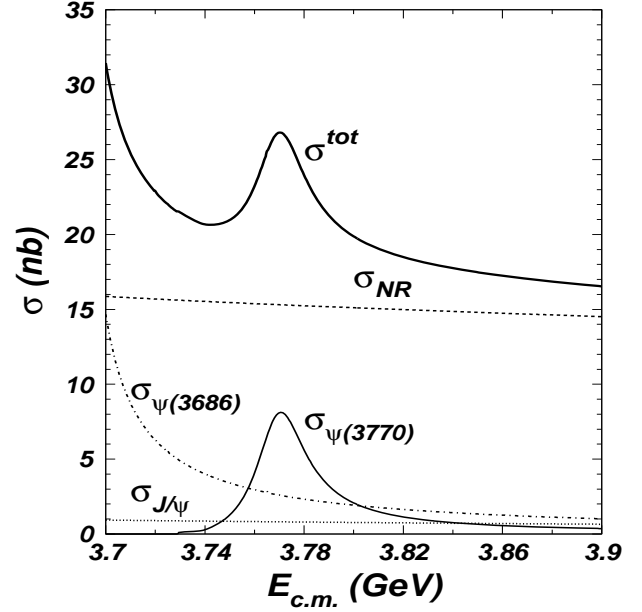


FIG. 4: The observed cross section in the vicinity of the  $\psi''$  resonance calculated with parameters provided by PDG. The total observed cross section  $\sigma^{tot}$  conventionally divided into four parts: the cross section from non resonant contribution  $\sigma_{NR}$ , from radiative tails of  $J/\psi$  ( $\sigma_{J/\psi}$ ) and  $\psi'$  ( $\sigma_{\psi'}$ ), and cross section from resonance  $\psi''$  ( $\sigma_{\psi''}$ ).

Fig. 4 draws diagrammatically the observed cross section in the vicinity of the  $\psi''$  resonance calculated with parameters provided by PDG [33]. The total observed cross section  $\sigma^{tot}$  is usually expressed as

$$\sigma^{tot} = \sigma_{NR} + \sigma_{J/\psi} + \sigma_{\psi'} + \sigma_{\psi''}, \quad (6)$$

which contains four parts: the non-resonance cross section  $\sigma_{NR}$ , the radiative tails of  $J/\psi$  ( $\sigma_{J/\psi}$ ) and  $\psi'$  ( $\sigma_{\psi'}$ ), and the  $\psi''$  resonance cross section ( $\sigma_{\psi''}$ ). The non-resonance cross section is usually expressed in terms of  $R$  value and the  $\mu$  pair cross section at Born order as  $\sigma_{NR} = R \cdot \sigma(e^+e^- \rightarrow \mu^+\mu^-)$ . The Breit-Wigner formula is adopted to depict the resonances of the  $J/\psi$ ,  $\psi'$  and  $\psi''$ , where the total decay width of the  $\psi''$  is energy dependent:

$$\sigma_{\psi''}(E_{c.m.}) = \frac{12\pi\Gamma_{ee}\Gamma_{\psi''}(E_{c.m.})}{(E_{c.m.}^2 - M_{\psi''}^2)^2 + \Gamma_{\psi''}^2(E_{c.m.})M_{\psi''}^2},$$

with

$$\Gamma_{\psi''}(E_{c.m.}) = C_{\Gamma} \left[ \frac{p_{D^0}^3}{1 + (rp_{D^0})^2} + \frac{p_{D^\pm}^3}{1 + (rp_{D^\pm})^2} \right], \quad (7)$$

where  $p$  is the  $D^0$  or  $D^\pm$  momentum,  $r$  is the classical

interaction radius, and  $C_\Gamma$  is defined as follows:

$$C_\Gamma \equiv \frac{\Gamma_{\psi''}(M_{\psi''})}{\left[ \frac{p_{D^0}^3}{1 + (rp_{D^0})^2} + \frac{p_{D^\pm}^3}{1 + (rp_{D^\pm})^2} \right] \Big|_{E_{c.m.}=M_{\psi''}}}.$$

Here  $\Gamma_{\psi''}(M_{\psi''})$  is the  $\psi''$  total decay width given by PDG [33]. The radiative correction scheme used by SPEAR experiment, is based on the work of Bonneau and Martin [34] and that of Jackson and Scharre [35]. The former only calculated to  $\alpha^3$  order which is insufficient for resonances; while the latter made some mistakes [36, 37]. The drawbacks due to the treatment of the radiative correction with these two schemes were studied for Z in Ref. [36] and for narrow resonances of  $\psi$  and  $\Upsilon$  families in Ref. [37]; but no such study on  $\psi''$  has been conducted so far. BES treats the radiative correction based on the structure function approach which achieves 0.1% accuracy [38]. The effect of the radiative correction can be seen from the ratio between the observed cross section  $\sigma^{obs}$  and the Born order cross section  $\sigma^{Born}$ , which is defined as

$$\sigma^{Born} = \frac{12\pi\Gamma_{ee}}{M_{\psi''}^2\Gamma_{\psi''}}.$$

From the last column of Table I, we see that the treatment of the radiative correction was consistent among different experiments at SPEAR. However, the resonance parameters from different experiments differ significantly. The reason remains unknown.

Another problem in previous analyses [15–18] is that the non- $D\bar{D}$  branching ratio was neglected in the fitting of the  $\psi''$  resonance curves. Since light hadrons have much lower thresholds than  $D\bar{D}$ , a larger non- $D\bar{D}$  branching ratio affects both directly the shape of the resonance curve and indirectly through the energy-dependent total width. Specially, taking into account the non- $D\bar{D}$  decays, Eq. (7) is revised by including another term, that is

$$\Gamma_{\psi''}(E_{c.m.}) = C'_\Gamma \times \left[ \frac{p_{D^0}^3}{1 + (rp_{D^0})^2} + \frac{p_{D^\pm}^3}{1 + (rp_{D^\pm})^2} + C_{\text{non-}D\bar{D}} \right],$$

where  $C_{\text{non-}D\bar{D}}$  is proportional to the partial width of the non- $D\bar{D}$  decays, and

$$C'_\Gamma \equiv \frac{\Gamma_{\psi''}(M_{\psi''})}{\left[ \frac{p_{D^0}^3}{1 + (rp_{D^0})^2} + \frac{p_{D^\pm}^3}{1 + (rp_{D^\pm})^2} + C_{\text{non-}D\bar{D}} \right] \Big|_{E_{c.m.}=M_{\psi''}}}.$$

With the  $C_{\text{non-}D\bar{D}}$  term in the expression for  $\Gamma_{\psi''}$ , the fitting of the resonance curve to extract the resonance parameters is done together with the fitting of the  $D\bar{D}$  or the non- $D\bar{D}$  cross section. In this procedure, the non- $D\bar{D}$  decay branching fraction is extracted together with the resonance parameters.

## B. Leading particle method

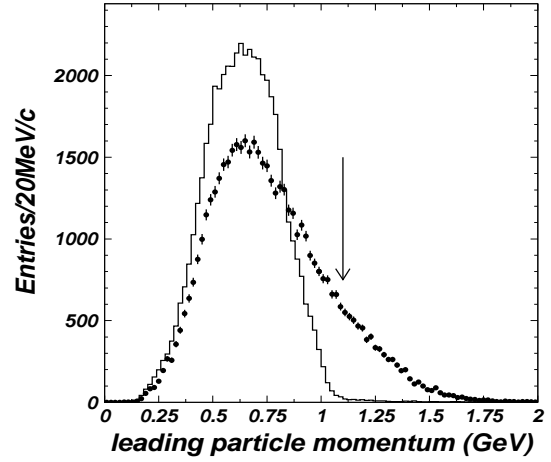


FIG. 5: Momentum distributions of the leading particle: histogram for  $D\bar{D}$  events; dots with error bars for  $D\bar{D}$ -less events (not normalized). The arrow indicates the cut at 1.1 GeV.

At first sight, it seems easy to measure the  $D\bar{D}$  cross section because the  $D\bar{D}$  decay has distinctive event topology and can be selected without ambiguity. But it is impractical for the scan experiment due to its low statistics. So we turn to the measurement of the  $D\bar{D}$ -less cross section, and take advantage of the salient kinetic feature of  $D\bar{D}$ -less decays, as mentioned in section IIIB for final state with  $K_S$ . This kinetic feature holds for all kinds of final states, which can be seen from a rough estimation. Since the mass of the  $\psi''$  is just above the  $D\bar{D}$ , the  $D$  and  $\bar{D}$  are almost static. Their decay products have momentum less than 932.3 MeV/c, which is half of the  $D^0$  mass. So the particles with momentum greater than this value must come from processes other than  $D$  or  $\bar{D}$  decays. With this distinction between  $D\bar{D}$  decay and  $D\bar{D}$ -less decay, we do not need the particle identification, but merely select the particle having the largest momentum, which is called the leading particle in a hadronic event. Fig. 5 shows the Monte Carlo simulation of the momentum distributions for the leading particle from  $D\bar{D}$  (denoted by histogram) and  $D\bar{D}$ -less decays (denoted by dot with error bar). It can be seen that the leading particles from  $D\bar{D}$  decay all have momentum less than 1.1 GeV. So a cut of  $p < 1.1$  GeV on momentum eliminates almost all events from  $D\bar{D}$  decays, while the surviving ones must come from  $D\bar{D}$ -less decays. This gives a direct measurement of  $D\bar{D}$ -less decay without the need to tag certain particle in the final states. We refer to this method as the **leading particle method**.

In the appendix, we present the formulae for  $\psi''$  scan. Based on these formulae, the expected cross sections in the vicinity of  $\psi''$  resonance are depicted and drawn in Fig. 6. The upper part of the graph is the total inclusive hadron cross section; while the lower part are the curves of cross sections from  $D\bar{D}$ -less decays, with the assump-

tion of non- $D\bar{D}$  decay branching fraction to be 0, 10% and 30%, respectively.

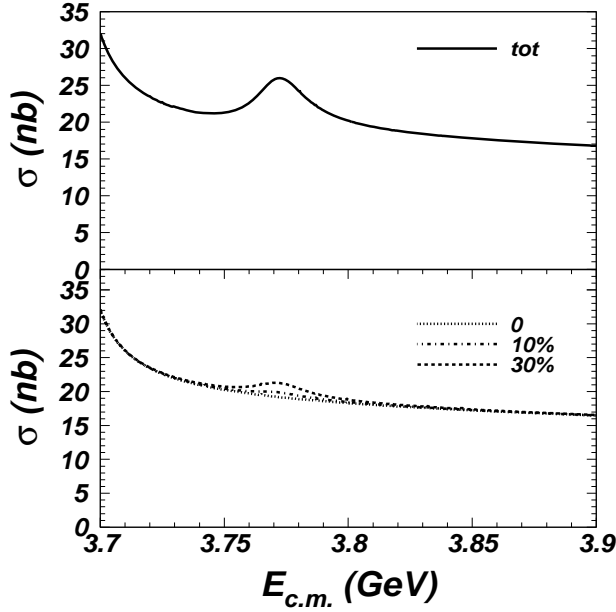


FIG. 6: The cross section in vicinity of the  $\psi''$  resonance calculated with parameters provided by PDG. In the top graph, the curve is the total cross section. In the bottom graph, only  $D\bar{D}$ -less decay cross section is drawn, with assumption of non-decay fraction as 0, 10% and 30%, respectively.

The prominent advantage of this method is the high sensitivity and good precision. Since the fraction of the non- $D\bar{D}$  decay is determined by the ratio of two curves from the same scan measurement, most of the systematic errors are canceled out, a small systematic uncertainty is expected from this method.

### C. Comments

Recently, CLEOc reported the measurement of non- $D\bar{D}$  cross section [39]:

$$\sigma_{n\bar{d}d} = (-0.01 \pm 0.08^{+0.41}_{-0.30})\text{nb} ,$$

which means the non- $D\bar{D}$  decays, even exist, are less than 0.69 nb at 90% confidence level, or correspond to an upper limit of 10.8% of the total decay width at 90% confidence level, if the total  $\psi''$  cross section is taken from the result by the same group  $\sigma_{\psi''} = (6.38 \pm 0.08^{+0.41}_{-0.30})\text{nb}$  [39].

Since non- $D\bar{D}$  searching is highly important and very interesting, so it is good to have other measurements by alternative methods to confirm this result. In addition, in the CLEOc analysis, the interference between resonance and continuum due to electromagnetic interaction is taken into account. To improve the accuracy further, other interference effects such as that between different resonances, need to be considered. The interference between strong decay process and non-resonance continuum

process may also give a non-vanishing contribution due to SU(3) flavor symmetry breaking. Although one may expect these interference effects to be negligible, more careful studies are needed to reduce the systematic uncertainties. We leave such meticulous analysis to a separate work in the future. Here we merely point out that the interference effect considered in Ref. [39] does not affect the measurement for non- $D\bar{D}$  decays by scan method suggested by us here as long as the  $\Gamma_{ee}$  of  $\psi'$  is treated as a free parameter in the data fitting. This is due to the fact that the interference term varies smoothly in the vicinity of  $\psi''$  peak.

## V. SUMMARY

In this paper, we put forth three methods for the searching for the non- $D\bar{D}$  decays of the  $\psi''$  in  $e^+e^-$  experiments: the exclusive, the quasi-inclusive and the inclusive methods.

First, for the exclusive method, we call attention on the contribution of the non-resonance virtual photon, and more importantly, its interference with the resonant decay amplitude. Besides the confirmation of the existence of the non- $D\bar{D}$  decays of the  $\psi''$ , the measurement of the exclusive channel is very important for the interpretation of the “ $\rho\pi$  puzzle” in  $J/\psi$  and  $\psi'$  decays and the determination of the phase between the strong and electromagnetic interactions in such decays.

Second, for the inclusive method, we propose a new, so-called leading particle method. This method tags a large fraction of the non- $D\bar{D}$  decays ( $\sim 10\%$ ) without  $D\bar{D}$  contamination, thus is more sensitive than the other methods in the determination of the total branching fraction of the non- $D\bar{D}$  decays of the  $\psi''$ .

As to the quasi-inclusive method, it can be used as a cross check for the measuring of the total branching fraction of the non- $D\bar{D}$  decays.

## Acknowledgments

This work is supported in part by the National Natural Science Foundation of China under Contract No. 10491303 and the 100 Talents Program of CAS under Contract No. U-25.

## APPENDIX: CROSS SECTION AT $\psi''$ MASS

The total cross section at the  $\psi''$  peak can be expressed as the sum of all possible resonances and non-resonance contributions. Due to Initial State Radiation (ISR) and other effects, such as energy spread, what is obtained experimentally is the so-called observed cross section instead of the one at Born order.

A remark of symbol is in order here. In the follow text, we use symbol  $W$  to denote the C.M. energy of

the colliding beams, which is also expressed by  $E_{c.m.}$  in the literature. The half of  $W$  indicates the beam energy, often written as  $E_{beam} = W/2$ , while the square of  $W$  indicates the energy transform, often written as  $s = W^2$  in theoretical papers.

## 1. ISR Correction

The ISR correction is calculated by the structure function approach [38, 40, 41], which yields the accuracy of 0.1%. In this scheme, the radiatively corrected cross section is expressed as

$$\sigma(W^2) = \int_0^{1-W_m^2/W^2} dx \tilde{\sigma}[W^2(1-x)]F(x, W) \quad (\text{A.1})$$

where  $W_m$  is the cut off of the invariant mass in the event selection, and

$$\tilde{\sigma}(W^2) = \frac{\sigma^B(W)}{|1 - \Pi(W^2)|^2},$$

with  $\sigma^B(W)$  the Born order cross section and  $\Pi(W^2)$  the vacuum polarization. In Eq. (A.1)

$$F(x, W) = \beta x^{\beta-1} \delta^{V+S}(W) + \delta^H(x, W), \quad (\text{A.2})$$

with

$$\beta = \frac{2\alpha}{\pi} \left( \ln \frac{W^2}{m_e^2} - 1 \right),$$

$$\delta^{V+S}(W) = 1 + \frac{3}{4}\beta + \frac{\alpha}{\pi} \left( \frac{\pi^2}{3} - \frac{1}{2} \right) + \beta^2 \left( \frac{9}{32} - \frac{\pi^2}{12} \right),$$

$$\delta^H(x, W) = -\beta \left( 1 - \frac{x}{2} \right) + \frac{1}{8}\beta^2 \left[ 4(2-x) \ln \frac{1}{x} - \frac{1+3(1-x)^2}{x} \ln(1-x) - 6+x \right].$$

Here the conversion of bremsstrahlung photons to real  $e^+e^-$  pairs is included in the cross section which is the usual experimental situation. Thus there is cancellation between the contributions of virtual and real  $e^+e^-$  pairs in the leading term [41].

The physical cross section at Born order of the process  $e^+e^- \rightarrow \text{Res.} \rightarrow f$  (where  $f$  denotes a certain kind of final states) is expressed by the **Breit-Wigner** formula

$$\sigma^{BW}(W) = \frac{12\pi\Gamma_{ee}^0\Gamma_f}{(W^2 - M^2)^2 + \Gamma^2 M^2},$$

where  $M$  and  $\Gamma$  are the mass and total width of the resonance;  $\Gamma_{ee}^0$  and  $\Gamma_f$  are the partial widths of the  $e^+e^-$  mode and the final state  $f$  respectively. Here  $\Gamma_{ee}^0$  describes the coupling strength of the resonance to  $e^+e^-$  through a virtual photon. For example, in potential

model,  $\Gamma_{ee}^0$  is related to the wave function at the origin  $\psi(0)$  in the way

$$\Gamma_{ee}^0 = \frac{4\alpha^2 Q_q^2 |\psi(0)|^2}{M^2},$$

where  $Q_q$  is the charge carried by the quark in the quarkonium and  $\alpha$  is the QED fine structure constant. Since the decay of a quarkonium  $1^{--}$  state to  $e^+e^-$  pair is through a virtual photon, there is always vacuum polarization associated with this process. So the experimentally measured  $e^+e^-$  partial width, denoted explicitly as  $\Gamma_{ee}^{exp}$ , is related to  $\Gamma_{ee}^0$  by the expression

$$\Gamma_{ee}^{exp} = \frac{\Gamma_{ee}^0}{|1 - \Pi(M^2)|^2}.$$

We follow the convention of Ref. [37] which is adopted by PDG. In this convention  $\Gamma_{ee}$  means  $\Gamma_{ee}^{exp}$ . For resonances, if they decay predominantly to light hadrons, with threshold ( $W_m$ ) far less than the data taking energy ( $W$ ), that is  $W - W_m \gg \Gamma$ , the integral of Eq. (A.1) is insensitive to  $W_m$ , because the Breit-Wigner formula behaves like a  $\delta$  function. One can put the upper limit of the integration to 1, so the radiatively corrected resonance cross section is

$$\sigma(W^2) = \int_0^1 dx F(x, W) \sigma^{BW}[W^2(1-x)], \quad (\text{A.3})$$

with

$$\sigma^{BW}(W) = \frac{12\pi\Gamma_{ee}\Gamma_f}{(W^2 - M^2)^2 + \Gamma^2 M^2}. \quad (\text{A.4})$$

## 2. Observed Cross Section

The total observed cross section  $\sigma^{tot}$  at the  $\psi''$  mass is usually expressed as

$$\sigma^{tot} = \sigma_{NR} + \sigma_{J/\psi} + \sigma_{\psi'} + \sigma_{\psi''}, \quad (\text{A.5})$$

which contains four parts: the cross section from non-resonant contribution  $\sigma_{NR}$ , from radiative tails of  $J/\psi$  ( $\sigma_{J/\psi}$ ) and  $\psi'$  ( $\sigma_{\psi'}$ ), and the cross section from resonance  $\psi''$  ( $\sigma_{\psi''}$ ).

### a. Non-resonance section

The non-charm contribution is conventionally expressed by R value

$$\sigma_{NR} = R \cdot \sigma(e^+e^- \rightarrow \mu^+\mu^-),$$

with

$$\sigma(e^+e^- \rightarrow \mu^+\mu^-) = \frac{4\pi\alpha}{3W^2}.$$

Here  $R$  indicates the contribution from light quarks[42] ( $u$ ,  $d$  and  $s$ ).



The resonances such as  $J/\psi$  and  $\psi'$ , are narrow with widths from tens to hundreds keV, while the beam energy spread of  $e^+e^-$  colliders is at the order of MeV. If the resonance width is comparable or smaller than the beam energy spread, the observed resonance cross section is the one by Eq. (A.1) folded with the beam energy spread function  $G(W, W')$ , which is usually taken as a Gaussian:

$$G(W, W') = \frac{1}{\sqrt{2\pi}\Delta} \exp \left[ -\frac{(W - W')^2}{2\Delta^2} \right],$$

with  $\Delta$  the standard deviation of the Gaussian distribution, or the beam energy spread physically. However, when the experiment energy is far from the resonance peak, the effect of the energy spread is insignificant and can be neglected[43].

As a matter of fact, Eq. (A.1) can further simplified. Notice that  $J/\psi$  and  $\psi'$  are narrow resonances, that is to say, comparing with the resonance mass  $M$ , the decay width  $\Gamma$  could be treated as  $\Gamma \rightarrow 0$ . So the Breit-Wigner formula transforms into a  $\delta$  function:

$$\sigma^{BW}(W) = \frac{12\pi\Gamma_{ee}\Gamma_f}{(W^2 - M^2)^2 + \Gamma^2 M^2}$$

$$\xrightarrow{\Gamma \rightarrow 0} \frac{12\pi^2\Gamma_{ee}B_f}{M} \cdot \delta(W^2 - M^2),$$

where  $B_f = \Gamma_f/\Gamma$ . Then the integral in Eq. (A.3) gives

$$\sigma(W^2) \cong \frac{12\pi^2\Gamma_{ee}B_f}{MW^2} \cdot F(x, W) \Big|_{x=1-\frac{M^2}{W^2}},$$

for the cross section due to the tails of the  $J/\psi$  and  $\psi'$ .

### c. Cross section of $\psi''$

According to Eq. (A.3), the radiatively corrected cross section of  $\psi''$  is expressed as

$$\sigma_{\psi''}(W) = \int_0^1 dx F(x, W) \sigma_{ND}[W^2(1-x)]$$

$$+ \int_0^{1-\frac{4m_{D^0}^2}{W^2}} dx F(x, W) \sigma_{DD}[W^2(1-x)],$$

where  $F(x, W)$  is given in Eq. (A.2), while

$$\sigma_{ND}(W^2) = \frac{12\pi\Gamma_{ee}\Gamma_{ND}}{(W^2 - M_{\psi''}^2)^2 + \Gamma_{\psi''}^2(W)M_{\psi''}^2}, \quad (\text{A.6})$$

and

$$\sigma_{DD}(W^2) = \frac{12\pi\Gamma_{ee}\Gamma_{DD}(W)}{(W^2 - M_{\psi''}^2)^2 + \Gamma_{\psi''}^2(W)M_{\psi''}^2}. \quad (\text{A.7})$$

The energy dependent total width of  $\psi''$  is composed of two parts

$$\Gamma_{\psi''}(W) = \Gamma_{ND} + \Gamma_{DD}(W), \quad (\text{A.8})$$

while the width listed by PDG is often defined as

$$\bar{\Gamma}_{\psi''} \equiv \Gamma_{\psi''}(W = M_{\psi''}). \quad (\text{A.9})$$

Using definition of Eq. (A.9), we further factorize the two decay widths in Eq. (A.8) as follows:

$$\Gamma_{ND} = f \cdot \bar{\Gamma}_{\psi''}, \quad (\text{A.10})$$

or

$$f = \frac{\Gamma_{ND}}{\bar{\Gamma}_{\psi''}},$$

that is to say,  $f$  is actually the branching fraction of the non- $D\bar{D}$  decays of  $\psi''$ . For  $\Gamma_{DD}$ , we have

$$\Gamma_{DD}(W) = (1-f) \cdot \bar{\Gamma}_{\psi''} \cdot \theta(W - 2m_{D^0}) \cdot$$

$$\frac{r_D \cdot \frac{p_{D^0}^3}{1 + (rp_{D^0})^2} + \theta(W - 2m_{D^\pm}) \cdot \frac{p_{D^\pm}^3}{1 + (rp_{D^\pm})^2}}{r_D \cdot \frac{\bar{p}_{D^0}^3}{1 + (r\bar{p}_{D^0})^2} + \frac{\bar{p}_{D^\pm}^3}{1 + (r\bar{p}_{D^\pm})^2}}, \quad (\text{A.11})$$

where  $r$  is the classical interaction radius;  $r_D$ , whose value is around 1.4, is the ratio of  $D^0\bar{D}^0$  to  $D^+D^-$  production at  $\psi''$  peak.  $p$  is the  $D^0$  or  $D^\pm$  momentum, reads explicitly as

$$p_{D^0} = \frac{1}{2}\sqrt{W^2 - 4m_{D^0}^2},$$

$$p_{D^\pm} = \frac{1}{2}\sqrt{W^2 - 4m_{D^\pm}^2};$$

and  $\bar{p}$  is the  $D^0$  or  $D^\pm$  momentum at the resonance peak, viz.

$$\bar{p}_{D^0} \equiv p_{D^0} \Big|_{W=M_{\psi''}} = \frac{1}{2}\sqrt{M_{\psi''}^2 - 4m_{D^0}^2},$$

$$\bar{p}_{D^\pm} \equiv p_{D^\pm} \Big|_{W=M_{\psi''}} = \frac{1}{2}\sqrt{M_{\psi''}^2 - 4m_{D^\pm}^2}.$$

### d. Cross section of the leading particle

The observed cross section at  $\psi''$  mass after requiring the momentum of the leading particle within certain ranges, which is denoted by  $\sigma^{l.p.}$  also contains four parts, i.e.

$$\sigma^{l.p.} = \sigma_{NR} + \sigma_{J/\psi} + \sigma_{\psi'} + \sigma_{\psi''}^{l.p.}.$$

Except for the last term, the other three parts are exactly the same as those of  $\sigma^{tot}$  in Eq.(6). As to  $\sigma_{\psi''}^{l.p.}$ , the radiatively corrected cross section reads

$$\sigma_{\psi''}^{l.p.}(W) = \int_0^1 dx F(x, W) \sigma_{ND}[W^2(1-x)],$$

where  $F(x, W)$  is given in Eq. (A.2), while  $\sigma_{ND}$  is given by Eq. (A.6).

The observed cross section of the  $D\bar{D}$  decays of  $\psi''$ , denoted as  $\sigma^{D\bar{D}}$ , which only comes from the resonance decays, is expressed as

$$\sigma_{\psi''}^{D\bar{D}}(W) = \int_0^{1 - \frac{4m_{D_0}^2}{W^2}} dx F(x, W) \sigma_{DD}[W^2(1-x)] ,$$

- 
- [1] E. Eichten *et al.*, Phys. Rev. Lett. **34**, 369 (1975); **36** (1976) 500; K. Lane and E. Eichten, *ibid.* **37** (1976) 477; **37** (1976) 1105(E).
- [2] E. L. Berger and C. Sorensen, Phys. Lett. B **62**, 303 (1976); D. P. Roy, Phys. Lett. B **62**, 315 (1976); J. Kwiecinski, Phys. Lett. B **72**, 245 (1977).
- [3] H. J. Lipkin, Phys. Lett. B **179**, 278 (1986); H. J. Lipkin, Nucl. Phys. B **244**, 147 (1984).
- [4] Yanong Zhu, Ph. D. thesis, California Institute of Technology, 1988, Caltech Report No. CALT-68-1513.
- [5] P. Wang, X. H. Mo and C. Z. Yuan, Phys. Rev. D **70**, 077505 (2004).
- [6] BES Collaboration, M. Ablikim *et al.*, Phys. Rev. D **70**, 077101 (2004).
- [7] BES Collaboration, M. Ablikim *et al.*, Phys. Rev. D **70**, 112007 (2004).
- [8] CLEO Collaboration, G. S. Adams *et al.*, Phys. Rev. D **73**, 012002 (2006).
- [9] CLEO Collaboration, T. E. Coan *et al.*, hep-ex/0509030.
- [10] CLEO Collaboration, G. S. Huang *et al.*, hep-ex/0509046.
- [11] J. Z. Bai, *et al.*, Phys. Lett. B **605**, 63 (2005).
- [12] CLEO Collaboration, N.E. Adam, hep-ex/0508023.
- [13] BES Collaboration, M. Ablikim *et al.*, Phys. Lett. B **603**, 130 (2004).
- [14] CLEO Collaboration, Q. He *et al.*, Phys. Rev. Lett. **95**, 121801 (2005).
- [15] P. A. Rapidis *et al.*, Phys. Rev. Lett. **39**, 526 (1977); I. Peruzz Phys. Rev. Lett. **39**, 1301 (1977); P. A. Rapidis [Lead-Glass-Wall Collaboration], "D Meson Production in  $e^+e^-$  Annihilation", Ph.D. Thesis, Stanford University, June 1979, SLAC-220/UC-34d(E).
- [16] W. Bacino *et al.*, Phys. Rev. Lett. **40**, 671 (1978).
- [17] R. H. Schindler *et al.*, Phys. Rev. D **21**, 2716 (1980); R. H. Schindler [MARK II Collaboration], "Charmed Meson Production and Decay Properties at the  $\psi''$ ", Ph.D. Thesis, Stanford University, May 1979, SLAC-219/UC-34d(T/E).
- [18] R. A. Partridge [Crystal Ball Collaboration], "A Study of the  $\psi''(3770)$  Using the Crystal Ball Detector", Ph.D. Thesis, California Institute of Technology, 1984, CALT-68-1150.
- [19] S. P. Chi [BES Collaboration], "Measurement of  $\psi''$  Resonance Parameters", Ph.D. Thesis, Institute of High Energy Physics, April 2003 (in Chinese).
- [20] J. L. Rosner, hep-ph/0405196.
- [21] BES Collaboration, J. Z. Bai *et al.*, Phys. Rev. Lett. **88**, 101802 (2002).
- [22] P. Wang, C. Z. Yuan and X. H. Mo, Phys. Rev. D **70**, 114014 (2004).
- [23] J. L. Rosner, Phys. Rev. D **64**, 094002 (2001).
- [24] P. Wang, C. Z. Yuan, X. H. Mo and D. H. Zhang, Phys. Lett. B **593**, 89 (2004).
- [25] P. Wang, X. H. Mo and C. Z. Yuan, Phys. Lett. B **574**, 41 (2003).
- [26] P. Wang, C. Z. Yuan and X. H. Mo, Phys. Rev. D **69**, 057502 (2004).
- [27] P. Wang, C. Z. Yuan and X. H. Mo, hep-ph/0512329.
- [28] D. L. Scharre *et al.*, Phys. Rev. Lett. **40**, 74 (1978).
- [29] MARK III Collaboration, R. M. Baltrusaitis *et al.*, Phys. Rev. Lett. **56**, 2140 (1986).
- [30] The detailed information about the simulation of inclusive hadronic event is provided in manual PYTHIA 6.3, hep-ph/0308153.
- [31] J.C. Chen *et al.*, Phys. Rev. D **62**, 034003 (2000).
- [32] J. Jadach, B.F.L. Ward and Z. Was, Phys. Rev. D **63**, 113009 (2001).
- [33] Particle Data Group, S. Eidelman *et al.*, Phys. Lett. B **592**, 1 (2004).
- [34] G. Bonneau and F. Martin, Nucl. Phys. B **27**, 381 (1971).
- [35] J. D. Jackson and D. L. Scharre, Nucl. Instrum. Methods **128**, 13 (1975).
- [36] J. P. Alexander *et al.*, Phys. Rev. D **37**, 56 (1988).
- [37] J. P. Alexander *et al.*, Nucl. Phys. B **320**, 45 (1989).
- [38] E. A. Kuraev and V. S. Fadin, Yad. Fiz. **41** (1985) 733 [Sov. J. Nucl. Phys. **41** (1985) 466].
- [39] CLEO Collaboration, D. Besson *et al.*, CLEO 05-27 (2005).
- [40] G. Altarelli and G. Martinelli, CERN **86-02** (1986) 47; O. Nicosini and L. Trentadue, Phys. Lett. **B196** (1987) 551.
- [41] F. A. Berends, G. Burgers and W. L. Neerven, Nucl. Phys. **B297** (1988) 429; *ibid.* **304** (1988) 921.
- [42] In the literature before,  $R_{charm}$  is introduced to depict the contribution from process  $e^+e^- \rightarrow \gamma^* \rightarrow D\bar{D}$ , However, for  $D\bar{D}$  final state, this process is indistinguishable from that of  $\psi''$  decay, therefore is unnecessary.
- [43] In our fitting program, when  $W \geq M_R + 0.2$  (GeV), the effect is neglected. So for our  $\psi''$  scan [ $W \subset (3.7, 3.9)$  GeV], the effect of energy spread is taken into consideration for  $\psi'$ , but not for  $J/\psi$ .